Proc. Natl. Acad. Sci. USA
Vol. 75, No. 3, pp. 1071–1075, March 1978
Biochemistry

Specific binding of $tRNA_f^{Met}$ to 23S rRNA of *Escherichia coli*

(initiator tRNA/hybridization/RNA–RNA interaction/tRNA unfolding)

JAMES E. DAHLBERG, CHRISTOPHER KINTNER*, AND ELSEBET LUND

Department of Physiological Chemistry, Medical Sciences Building, University of Wisconsin, Madison, Wisconsin 53706

Communicated by Philip P. Cohen, November 11, 1977

ABSTRACT **$tRNA_f^{Met}$ binds to 23S rRNA of *Escherichia coli*, forming a complex with a melting temperature of 75° (in 0.6 M NaCl). The regions within the RNAs that bind to each other have been isolated and their nucleotide sequences have been determined. The interacting region in $tRNA_f^{Met}$ is 17 nucleotides long, extending from G_5 in the acceptor stem to D_{21} (D = 5,6-dihydrouridine) in the D loop. The sequence in 23S rRNA is complementary to that sequence except for an extra Up in the middle and allowing a Gp·D base pair. We propose that association of these two sequences may play a role in initiation of protein synthesis by $tRNA_f^{Met}$. In addition, part of this sequence in 23S rRNA may also stabilize tRNA binding to the ribosome during elongation of nascent polypeptides.**

Several biologically important processes are mediated through RNA–RNA interactions. For example, steps of protein synthesis involving recognition of one RNA sequence by another include mRNA binding to 30S ribosomal subunits, codon–anticodon recognition, tRNA binding to ribosomes (via 5S rRNA), and perhaps 50S–30S ribosomal subunit association (1–4).

We have previously observed that several tRNAs of *Escherichia coli* can associate with ribosomal RNAs (5). Some of the complexes formed are much more stable than others.

In this report we describe the association of $tRNA_f^{Met}$ with 23S rRNA of *E. coli*. The binding occurs between complementary regions of the two RNAs. In the case of $tRNA_f^{Met}$, the binding region is 17 nucleotides long, extending from the 5′ side of the acceptor stem through most of the D stem and loop. It is possible that this interaction plays a role in the alignment of 50S ribosomal subunits on 30S subunit–$tRNA_f^{Met}$ complexes during initiation of protein synthesis. Furthermore, because part of the binding region in 23S rRNA is complementary to invariant nucleotides in the D-loop of tRNAs (6, 7), it might also interact with tRNAs during elongation of nascent polypeptide chains.

MATERIALS AND METHODS

30S [^{32}P]rRNA of *E. coli* was prepared as described elsewhere (5) from AB301/105 cells labeled in the presence of chloramphenicol. 4S [^{32}P]RNA was isolated by hot sodium dodecyl sulfate lysis (2×10^9 cells/ml in 0.5% sodium dodecyl sulfate/0.1 M NaCl/20 mM EDTA/10 mM Tris·HCl, pH 7.5; 100° for 90 sec) and phenol extraction of CP78 or MRE600 cells grown in the presence of $^{32}PO_4^{3-}$. Unlabeled 16S and 23S rRNAs were isolated by phenol extraction of purified 30S and 50S ribosomal subunits of MRE600 cells, followed by centrifugation in 18-ml gradients of 5–20% sucrose/0.1% Sarkosyl/TSE buffer (0.01 M Tris·HCl, pH 7.6/0.15 M NaCl/0.0015 M EDTA) at 4° for 18 hr at 24,000 rpm in a Beckman SW 27.1 rotor.

Unlabeled $tRNA_f^{Met}$ was purchased from Boehringer Mannheim. [^{32}P]$tRNA_f^{Met}$ was prepared by two-dimensional gel electrophoresis of gradient-purified 4S RNA (see Fig. 1*B*). The region of the gel containing $tRNA_f^{Met}$ was excised and used as the origin for a third dimension of electrophoresis, in 15% polyacrylamide/7 M urea/TEB buffer (89 mM Tris/2.8 mM EDTA/89 mM boric acid, pH 8.3) (8). After electrophoresis for 20 hr at 400 V, 15°, the RNA was located by autoradiography, eluted, and characterized by oligonucleotide fingerprinting.

Complexes between rRNAs and 4S RNAs were prepared by heating the RNAs in binding buffer (0.02 M Tris·HCl, pH 7.6/0.6 M NaCl/0.02 M EDTA) to 85–90° for 5 min, annealing at 65–67° for 30–60 min, and quenching on ice. Depending on the amount of 23S rRNA in the reaction (usually held at 0.1–0.4 mg/ml), the reaction volume was varied between 10–100 μl. The amounts of tRNAs added were calculated to have $tRNA_f^{Met}$ in 2- to 10-fold molar excess over 23S rRNA.

Complexes were separated from unbound 4–5S RNA by centrifugation in a 5-ml 5%–20% sucrose gradient in 0.1% Sarkosyl, TSE buffer at 4° for 3½ hrs at 49,000 rpm in a Beckman SW 50.1 rotor. Ten-drop fractions were collected and appropriate peaks were pooled, yeast carrier RNA was added (to 50 μg/ml), and the RNA was precipitated by 2½ volumes ethanol.

In the protection experiments, complexes were resuspended in diluted (1/2) binding buffer and sufficient RNase T1 (Calbiochem) and pancreatic RNase (Worthington) were added to make the final weight ratios of RNA to each enzyme 10:1. Digestions were carried out at 20° for 30 min followed by digestion with Pronase at 1 mg/ml (30 min, 37°), phenol extraction, and ethanol precipitation. When the protected complex was labeled in 23S rRNA, the labeled fragment was rehydridized to unlabeled $tRNA_f^{Met}$, as above, prior to electrophoresis (see legend to Fig. 5); when the complex was labeled in $tRNA_f^{Met}$, it was applied directly to the gel, after resuspension of the ethanol precipitate. Electrophoresis was in 20% polyacrylamide in diluted (1/2) TEB buffer for 6 hr at 400 V, 15° in an E-C model 470 vertical slab gel electrophoresis cell.

Two-dimensional polyacrylamide gel electrophoresis, two-dimensional paper electrophoretic analysis of oligonucleotides (fingerprinting) and analysis of purified oligonucleotides were carried out as described elsewhere (9–11). Silkworm nuclease, provided by A. Mukai, was used at 0.2 units/ml in 0.1 M NaCl/0.5 mM $Mg(OAc)_2$/0.05 M Na_2CO_3, pH 10.5 for 2 hr at 37°; resulting products, which had either a 5′-phosphate or 5′-hydroxyl group (arising internally or at the 5′ end of the oligonucleotides, respectively) were separated by electrophoresis at pH 3.5 on DEAE-cellulose paper, and further analyzed by RNase T2 and venom phosphodiesterase digestion, followed by two-dimensional thin-layer chromatography (12).

The costs of publication of this article were defrayed in part by the payment of page charges. This article must therefore be hereby marked "*advertisement*" in accordance with 18 U. S. C. §1734 solely to indicate this fact.

Abbreviations: TSE, Tris/saline/EDTA buffer; TEB, Tris/EDTA/boric acid buffer; D, 5,6-dihydrouridine.

* Present address: McArdle Laboratory for Cancer Research, University of Wisconsin, Madison, WI 53706.

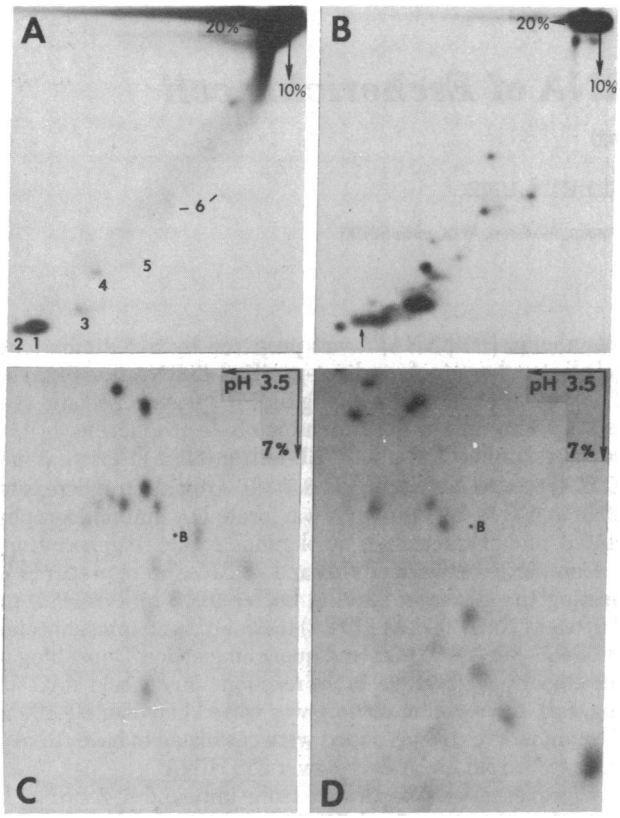

FIG. 1. Characterization of small RNAs associated with *E. coli* 30S rRNA. Autoradiograms of two-dimensional polyacrylamide gel electrophoresis patterns (11) are shown. (*A*) Small RNAs released from ^{32}P-labeled 30S rRNA by heating of the RNA to 85–90° prior to loading on the gel; (*B*) total 4–8S RNAs of *in vivo* ^{32}P-labeled logarithmic-phase AB301/105 cells. The RNAs of spots 1–6 in *A* were identified as $tRNA_{f3}^{Met}$, $tRNA_{f1}^{Met}$, $tRNA_1^{Asp}$, $tRNA_1^{Leu}$, $tRNA_3^{Ser}$, and 5S rRNA, respectively, using oligonucleotide fingerprint analysis (10, 11) of RNase T1 digests of these RNAs. The arrow in *B* indicates the position of $tRNA_{f3}^{Met}$ (spot 1 in *A*) in total *E. coli* 4S RNA. (*C* and *D*) Autoradiograms of fingerprints obtained after digestion of $tRNA_{f3}^{Met}$ (spot 1 RNA of *A*) with RNase T1 or pancreatic RNase, respectively. B marks the position of xylene cyanol FF blue dye.

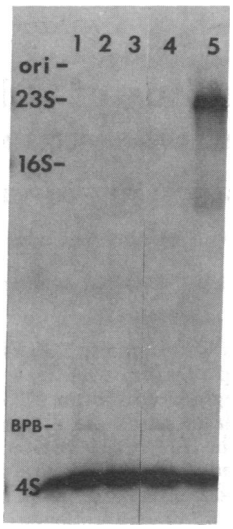

FIG. 2. Formation of $tRNA_f^{Met}$–rRNA complexes. ^{32}P-Labeled $tRNA_f^{Met}$ was electrophoresed in a 2.5% polyacrylamide/0.5% agarose gel alone (slot 1) or mixed with unlabeled 16S rRNA (slots 2 and 3) or unlabeled 23S rRNA (slots 4 and 5). Prior to electrophoresis, the samples in slots 3 and 5 were incubated at 70° for 30 min, whereas those in slots 1, 2, and 4 were kept at 0°. Each 15-μl sample contained about 2000 cpm of [^{32}P]$tRNA_f^{Met}$ and 0.2 mg of rRNA per ml, as appropriate. An autoradiograph of the gel is shown; the positions of 16S and 23S rRNAs, determined by staining of the gel with Stains-All (16) prior to drying and autoradiography, are indicated. ori and BPB show the positions of the origin and bromophenol blue dye marker. 4S denotes location of nonhybridized tRNA.

RESULTS

Identification of Complexed RNAs. We previously observed that brief heat treatment of 30S rRNA led to the release of several associated 4–5S RNAs (5). As shown in Fig. 1*A*, the two-dimensional gel electrophoresis pattern of these released small RNAs was considerably simpler than the pattern of total 4–5S RNAs (Fig. 1*B*). The released small RNAs were eluted from the gel and identified by oligonucleotide fingerprint analysis. The RNase T1 and pancreatic RNase digestion oligonucleotides of the RNAs of spots 1 (Fig. 1 *C* and *D*, respectively) and 2 were those of $tRNA_f^{Met}$ (13). The fingerprints differed from each other by the presence of oligonucleotides containing m^7Gp ($tRNA_{f3}^{Met}$) or Ap ($tRNA_{f1}^{Met}$), which are at position 47 of the RNAs (spots 1 and 2 of Fig. 1*A*, respectively) (14). These assignments were confirmed by redigestion of all oligonucleotides by pancreatic RNase or RNase T1, as appropriate. Other associated RNAs were identified as $tRNA_1^{Asp}$ (spot 3), $tRNA_1^{Leu}$ (spot 4), $tRNA_3^{Ser}$ (spot 5), and 5S rRNA (spots 6). Although interaction between 5S rRNA and 23S rRNA has been described by others (15), there have been no reports of binding of specific tRNAs to rRNAs.

The relative amounts of the various RNAs bound to 30S rRNA were determined by quantitation of radioactivity in the various spots. Of the associated small RNAs, more than 80% were $tRNA_f^{Met}$. Because of the predominance of $tRNA_f^{Met}$, we elected to study its association with rRNA in detail.

The part of the 30S rRNA to which $tRNA_f^{Met}$ bound was determined by hybridizing ^{32}P-labeled $tRNA_f^{Met}$ to various purified unlabeled rRNAs. After hybridization, the RNAs were analyzed by one-dimensional electrophoresis in a polyacrylamide/agarose composite gel. An autoradiogram of such an analysis (Fig. 2) showed that $tRNA_f^{Met}$ hybridized to 23S rRNA but not to 16S rRNA or 5S rRNA (not shown). Quantitation of the amount of radioactive $tRNA_f^{Met}$ in the complexes relative to the amount of 23S rRNA indicated that about one molecule of tRNA was bound per 23S rRNA molecule.

When 23S rRNA was isolated from cells by the hot sodium dodecyl sulfate extraction procedure used to isolate 30S rRNA, $tRNA_f^{Met}$ was associated with it. In contrast, when the 23S rRNA was isolated from purified 50S ribosomal subunits, no significant amounts of $tRNA_f^{Met}$ were bound (data not shown). Thus, the association of $tRNA_f^{Met}$ with 30S (and 23S) rRNA could well have occurred during cell lysis and extraction of the RNAs at elevated temperatures.

Stability of the $tRNA_f^{Met}$–23S rRNA Complex. The stability of the interaction between $tRNA_f^{Met}$ and 23S rRNA was determined by measuring the melting temperature of gradient-purified complex labeled only in $tRNA_f^{Met}$. Aliquots of the complex were heated for 5 min at the indicated temperatures, rapidly chilled on ice, and assayed by gel electrophoresis. The results in Fig. 3 showed that 50% of the complex was dissociated by heating to 75° in 0.6 M NaCl. Comparable measurements for the other associated tRNAs showed that the melting temperatures of those complexes were at least 5° below that of the $tRNA_f^{Met}$ complex (our unpublished observations).

Interacting Nucleotide Sequences in the Complex. The region of $tRNA_f^{Met}$ that interacted with 23S rRNA was identified

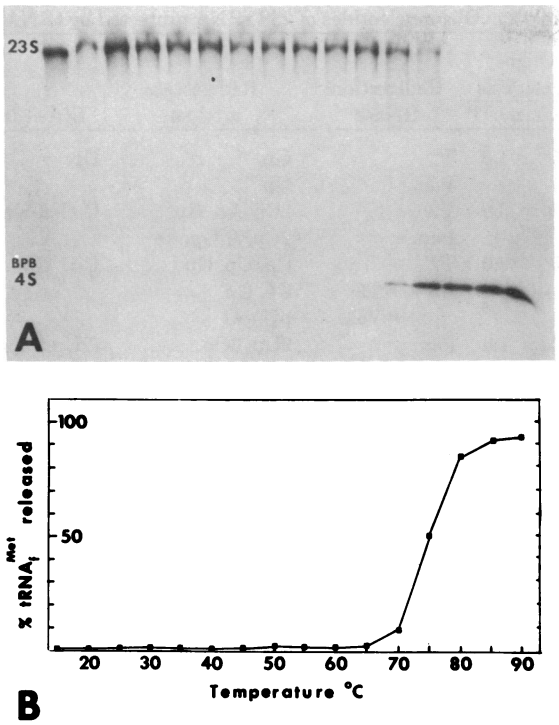

FIG. 3. Determination of the melting temperature of the tRNA$_f^{Met}$–23S rRNA complex. (*A*) Autoradiogram of a 2.5% polyacrylamide/0.5% agarose composite gel containing samples of gradient-purified ^{32}P-labeled tRNA$_f^{Met}$–23S rRNA complex which had been heated for 5 min at the temperatures indicated in *B* and then quenched on ice. Each sample contained 1 μg of 23S rRNA and 1500 cpm of [^{32}P]tRNA$_f^{Met}$ in 5 μl of binding buffer. The position of 23S rRNA in the gel was located by staining (16). The melting temperature of the tRNA$_f^{Met}$–23S mRNA complex was determined by measuring for each slot the radioactivity in the 23S rRNA region and in the tRNA$_f^{Met}$ region of the gel and calculating the percentage of the total radioactivity of each sample found in the tRNA$_f^{Met}$ region. The results are shown in *B* as percent tRNA$_f^{Met}$ released versus temperature of incubation. A melting temperature of 75° was obtained for the complex.

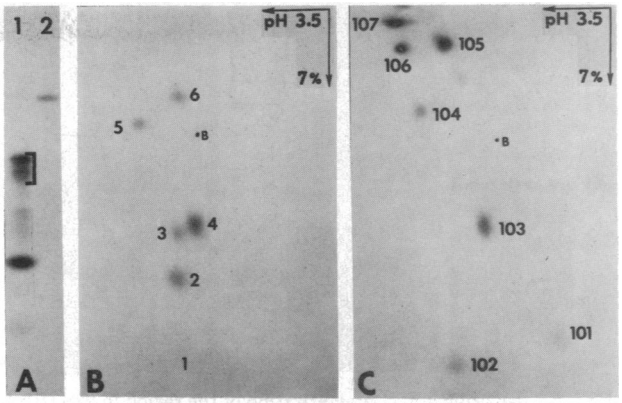

FIG. 4. Isolation and characterization of the region in tRNA$_f^{Met}$ that binds 23S rRNA [^{32}P]tRNA$_f^{Met}$ was hybridized to unlabeled 23S rRNA and the complex was digested with a mixture of RNase T1 and pancreatic RNase. (*A*) Autoradiogram of a one-dimensional 20% polyacrylamide gel containing in slot 1 RNase-treated tRNA$_f^{Met}$–23S rRNA complex, which was labeled with ^{32}P in the tRNA$_f^{Met}$, and in slot 2 untreated, full-length ^{32}P-labeled tRNA$_f^{Met}$. No bands were observed when uncomplexed tRNA$_f^{Met}$ was digested. The complex-specific RNase-resistant fragments indicated by the bracket in slot 1 were eluted and the protected region of tRNA$_f^{Met}$ was characterized by oligonucleotide fingerprint analyses. Autoradiograms of the RNase T1 and pancreatic RNase fingerprints are shown in *B* and *C*, respectively. The numbering system used in analysis of individual oligonucleotides (see Table 1) is indicated.

by digestion of the complex containing unlabeled 23S rRNA and [^{32}P]tRNA$_f^{Met}$ with RNase T1 plus pancreatic RNase, under conditions where RNA·RNA duplexes would not be digested. As seen in Fig. 4*A*, RNase-resistant fragments of RNA (denoted by a bracket in slot 1) could be detected after polyacrylamide gel electrophoresis. These bands were observed only when tRNA$_f^{Met}$ and 23S rRNA were annealed to each other prior to digestion (data not shown). The RNase-resistant fragments were eluted from the gel and digested under standard conditions with either RNase T1 (Fig. 4*B*) or pancreatic RNase (Fig. 4*C*), and the resulting oligonucleotides were separated by fingerprinting. Each oligonucleotide was subsequently characterized by redigestion with other RNases as appropriate; the results, listed in Table 1, indicated that the protected fragment extended from position 5 to position 21 from the 5′ end of tRNA$_f^{Met}$, as sequenced by Dube *et al.* (14) (see also Fig. 6).

The region of 23S rRNA to which tRNA$_f^{Met}$ bound was isolated in a way analogous to that described above for the tRNA$_f^{Met}$ fragment. In this case, ^{32}P-labeled 23S rRNA was hybridized to unlabeled tRNA$_f^{Met}$ and the complex was digested with a mixture of RNase T1 and pancreatic RNase. In order to facilitate separation of the tRNA$_f^{Met}$-protected fragment from the bulk of 23S rRNA digestion products, the fragment was rehybridized to unlabeled tRNA$_f^{Met}$ as described in the legend to Fig. 5. The 23S rRNA-derived fragments were then isolated complexed to the 4S tRNA$_f^{Met}$, as shown in Fig. 5*A*. From this figure it is clear that fragment production required hybridization of 23S [^{32}P]rRNA to tRNA$_f^{Met}$ prior to nuclease digestion (compare slots 3 and 4 in Fig. 5*A*). Several bands were observed

Table 1. Oligonucleotides of tRNA$_f^{Met}$ protected by 23S rRNA

Oligonucleotide No.	mol P	Redigestion RNase	Redigestion products	Structures
1	0.3	T2	Dp	Dp
2	5.6	T2	Gp	Gp
3	2.2	T2	Ap, Gp	A-Gp
		Pan.	A-Gp	
4	3.0	T2	Cp, Ap, Gp	C-A-Gp
		Pan.	Cp, A-Gp	
5	2.0	T2	Up, Gp	U-Gp
		Pan.	Up, Gp	
6	4.6	T2	2Cp, Up, Gp	[C-C-U-]Gp
		Pan.	2Cp, Up, Gp	
101	0.9	T2	Cp	Cp
102	0.6	T2	Up	Up
103	3.0	T2	Ap, Gp, Cp	[A-G-]Cp
104	0.8	T2	Gp	G-Gp
105	5.3	T2	Ap, 3Gp, Cp	[G-G-A-G-]Cp
106	2.2	T2	2Gp, Dp	G-G-Dp
107	3.0	T2	3Gp, Up	G-G-G-Up

Oligonucleotides shown in Fig. 4 *B* and *C* were characterized by quantitation of radioactivity and redigestion after elution from the paper, using standard methods (11, 14). Sequences were deduced from these results and the positions of the oligonucleotides on the fingerprints. The relative numbers of phosphates in oligonucleotides 1–6 (RNase T1 products) and 101–107 (pancreatic RNase products) were normalized to 3.0 mol of phosphate in oligonucleotides 4 and 103, respectively. The relative yields of redigestion products were approximated by inspection of autoradiograms. Structures shown in brackets were deduced from the composition of the oligonucleotide and from the known sequence of tRNA$_f^{Met}$. Pan., pancreatic RNase; T2, RNase T2; D, 5,6-dihydrouridine.

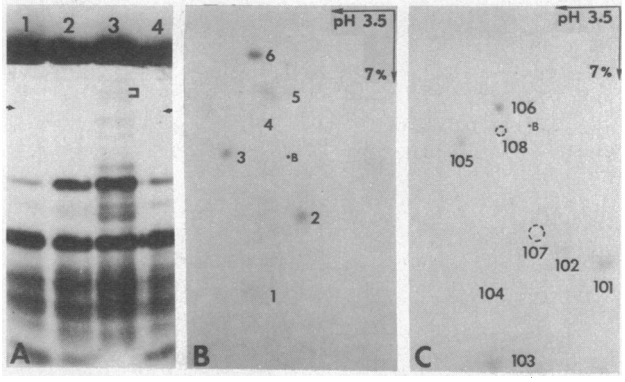

FIG. 5. Isolation and characterization of the region in 23S rRNA that binds $tRNA_f^{Met}$. 23S [^{32}P]rRNA was hybridized to unlabeled $tRNA_f^{Met}$ and the complex was digested with a mixture of RNase T1 and pancreatic RNase. (*A*) Autoradiogram of a 20% polyacrylamide gel analysis of the RNase-resistant fragments of 23S rRNA. The samples in slots 1 and 2 contained no $tRNA_f^{Met}$ during the digestion, whereas those in slots 3 and 4 contained 15 μg of $tRNA_f^{Met}$. Samples 2 and 3 were hybridized prior to digestion, whereas samples 1 and 4 were not. Prior to electrophoresis, but after nuclease digestion, all four samples were hybridized to 5 μg of added unlabeled $tRNA_f^{Met}$. The position of unlabeled $tRNA_f^{Met}$ after electrophoresis was determined by staining (16) and is indicated by the arrows in slots 1 and 4. All bands present only in slot 3 were eluted and fingerprinted. (*B* and *C*) Autoradiograms of fingerprints of RNase T1 and pancreatic RNase digests, respectively, of the band indicated by the bracket in slot 3 of *A*. The numbering system used in analysis of oligonucleotides (see Table 2) is indicated; in addition, the location of two oligonucleotides present in digests of some fragments but not the one shown here are indicated by broken circles in *C*.

after gel electrophoresis (slot 3 in Fig. 5 *A*): structural analyses of the 23S-RNA fragments in these bands showed that they differed in their 5′ and 3′ ends (see below).

The sequences of the protected fragments derived from 23S rRNA were determined by digestion with RNase T1 or pancreatic RNase. Fig. 5 *B* and *C* shows the fingerprints of the fragment indicated by the bracket in Fig. 5*A*, slot 3. The sequences of most of the oligonucleotides could be deduced directly from the structures of redigestion products, as listed in Table 2. In the case of oligonucleotide 6, complete sequence analysis required partial digestion with silkworm nuclease. The products produced by this enzyme were then analyzed by digestion with RNase T2 or venom phosphodiesterase, as indicated in Table 2. From the products listed in Table 2 it is possible to reconstruct only one sequence of the major 23S rRNA-derived protected fragment, *viz.*, C-C-A-G-G-C-U-G-U-C-U-C-C-A-C-C-C-Gp. The 3′ decanucleotide of the sequence has been shown by Branlant *et al.* (17) to be derived from a region between 900 and 990 nucleotides from the 3′ end of 23S rRNA.

Several oligonucleotides were present in fingerprints of some but not all of the fragments (e.g., 107 and 108 of Fig. 5*C* and Table 2). These products presumably resulted from partial RNase resistance of the ends of the complexed regions. From these products the sequence can be extended by two Gp residues at the 5′ end. As shown in the bottom of Fig. 6, the 23S rRNA sequence is complementary to the protected $tRNA_f^{Met}$ sequence, allowing for the looping out of one Up and the formation of a D·G base pair.

DISCUSSION

In this report we describe a novel association between RNA components of the protein synthesis apparatus of *E. coli*: the binding of $tRNA_f^{Met}$ to 23S rRNA. Because of the low probability

Table 2. Oligonucleotides of 23S rRNA protected by $tRNA_f^{Met}$

Oligonucleotide No.	mol P	Redigestion RNase	Redigestion products	Structures
1	1.8	T2	Gp	Gp
		Pan.	Gp	
2	3.8	T2	2Cp, Ap, Gp	C-C-A-Gp
		Pan.	2Cp, A-Gp	
3	3.0	T2	Cp, Up, Gp	C-U-Gp
		A.P. → T2	Cp, Up	
		→ Ven.	pU, pG	
4	1.0	Pan.	2Up, 3Cp	(2Up,3Cp)
5	2.5	Pan.	A-Cp, 4–5Cp, 2Up	(2Up,3Cp)-
		U2 → T2	(2Up,3Cp)Ap	A-C-C-Cp
		U2 → T2	3Cp	
6	6.8	Pan.	A-Cp, 2Up, 4–5Cp, Gp	U-C-U-C-C-A-C-C-C-Gp
		U2 → T2	3Cp, Gp	C-C-C-Gp
		U2 → T2	(2Up,3Cp)Ap	(2Up,3Cp)Ap
		S.W. → T2	Up	U-C
		→ Ven.	pC	
		S.W. → T2	Up, Cp	U-C-U
		→ Ven.	pC, pU	
		S.W. → T2	2Up, Cp	U-C-U-C
		→ Ven.	2pC, pU	
		S.W. → T2	2Up, 2Cp	U-C-U-C-C
		→ Ven.	3pC, pU	
		S.W. → T2	pUp, 2Cp	pU-C-C-A
		→ Ven.	2pC, pU, pA	
101	5.8	T1	Cp	Cp
		T2	Cp	
102	1.6	T1	Ap, Cp	A-Cp
		T2	A-Cp	
103	2.2	T1	Up	Up
		T2	Up	
104	0.3	T1	Gp	Gp
105	1.9	T1	Gp, Up	G-Up
		T2	Gp, Up	
106	4.0	T1	A-Gp, Gp, Cp	A-G-G-Cp
		A.P. → T2	Ap, 2Gp	
		→ Ven.	2pG, pC	
107	1.0	T2	Gp, Cp	G-Cp
108	0.8	T2	2Gp, Cp	G-G-Cp

Oligonucleotides shown in Fig. 5 *B* and *C* were characterized as described in Table 1. Radioactivity in RNase T1 oligonucleotides (1–6) was normalized to 3.0 phosphates in oligonucleotide 3, whereas radioactivity in the pancreatic RNase oligonucleotides (101–108) was normalized to 4.0 phosphates in oligonucleotide 106. The numbers are the averages of 8 determinations (1–6) or 4 determinations (101–108). T2, RNase T2; Pan., pancreatic RNase; T1, RNase T1; A.P., bacterial alkaline phosphatase; Ven., snake venom phosphodiesterase; S.W., silkworm nuclease. C-C-C-Gp obtained by digestion of oligonucleotide 6 with U2 RNase was further characterized by coelectrophoresis (DEAE-cellulose DE 81 paper, pH 3.5) with authentic C-C-C-Gp (obtained by RNase T1 digestion of *E. coli* $tRNA_2^{Glu}$).

of such a complementarity of sequences, it is very tempting to attribute some functional significance to the interaction. For example, it may facilitate the correct alignment of 30S ribosome–mRNA–$tRNA_f^{Met}$ complexes onto 50S ribosomes (18) during initiation of protein synthesis. Alternatively, the binding of $tRNA_f^{Met}$ to 23S rRNA may somehow control ribosome synthesis or assembly, or modulate the activity of RNA polymerase.

At present, we have no evidence to support or rule out any of these models, nor can we even say that the binding is physi-

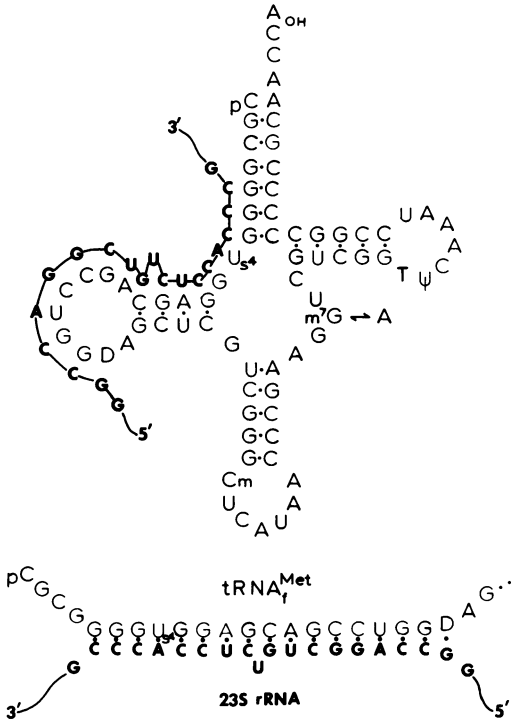

FIG. 6. Sequences involved in formation of the complex between 23S rRNA and tRNA$_f^{Met}$. The upper part of the figure shows the cloverleaf model of *E. coli* tRNA$_f^{Met}$ (14) with the complementary 23S rRNA sequence aligned to indicate where interaction between the two molecules could occur. The lower part of the figure shows the nucleotide sequences obtained from the RNase-resistant (double-stranded) region of the tRNA$_f^{Met}$–23S rRNA complex (see also Tables 1 and 2). The interacting region of the 23S rRNA has been localized in section R between 900 and 990 nucleotides from the 3′ end of 23S rRNA according to the oligonucleotide maps obtained by Branlant *et al.* (17).

ologically significant. 23S rRNA, as it is isolated from purified 50S ribosomal subunits, contains no detectable tRNA$_f^{Met}$ bound to it (our unpublished observations). Perhaps the intracellular association between tRNA$_f^{Met}$ and 23S rRNA is sufficiently transient or unstable as to escape detection by the methods employed by us here.

It may well be that the entire length of the complementary sequences between 23S rRNA and tRNA$_f^{Met}$ never exists as a duplex, as that would require considerable unfolding of the tRNA (see Fig. 6). Crothers *et al.* (19) reported that the base-pairing in the D-stem and the interaction between loops I and IV (the D- and T-Ψ-C-G-loops, respectively) are the least stable interaction in tRNA$_f^{Met}$, melting at about 46° in 0.17 M NaCl, no Mg^{2+}. This relative instability could facilitate base pairing between 23S rRNA and nucleotides in the D-loop or D-stem.

In this regard it is interesting that the "invariant" nucleotides A_{14}, G_{18}, and G_{19}, which are present in both initiator and elongation tRNAs, might become accessible to interaction with 23S rRNA during binding of any tRNA to ribosomes. Dube (20) and Erdmann (4) have presented evidence that the G-T-Ψ-C sequence in loop IV basepairs with a complementary sequence in 5S rRNA; such binding could occur only if the loop I–loop IV interactions seen in the crystal structure of yeast tRNA^{Phe} (6, 7) were disrupted. Thus, the interaction seen here between a specific region of 23S rRNA and the D-loop of tRNA$_f^{Met}$ may also function in stabilizing the binding of all tRNAs to ribosomes during protein biosynthesis. These other D-loop–23S rRNA interactions would be shorter than that between tRNA$_f^{Met}$ and 23S rRNA, and thus would not be detected by our methods. It should, however, be noted that the interacting region of 23S rRNA (Fig. 6) is inaccessible to reaction with kethoxal, at least in isolated 50S ribosomal subunits, and in the absence of tRNA (21).

Analyses of the RNase-resistant fragments of tRNA$_f^{Met}$–23S rRNA complexes reveal some heterogeneity at the ends, probably caused by breathing at the ends of the duplex. Interestingly, when the 23S rRNA-derived fragment is isolated after digestion with RNase T1 and pancreatic RNase, over half of the fragments still have a 3′-Gp on oligonucleotide 6 (the 3′ end), although there is no Cp in the complementary part of tRNA$_f^{Met}$. Furthermore, the protected fragment often contains two additional Gp residues at its 5′ end, which might afford partial protection of the Dp at the 3′ end of the tRNA$_f^{Met}$ fragment (or of the pyrimidines in other tRNAs). Even though a Up residue is looped out of the middle of the double-stranded duplex, we are able to recover the strand intact. We attribute that to partial resistance of the looped-out nucleotide to digestion with pancreatic RNase, and to the fact that we undoubtedly select for intact fragments by the second hybridization during purification.

This work was supported by Grants GB32152X and PCM77-07357 from the National Science Foundation. We thank B. P. Stark for technical assistance, S. Meier and D. Hoover for typing the manuscript, and Dr. A. E. Dahlberg for reading the manuscript.

1. Kurland, C. G. (1977) *Annu. Rev. Biochem.* **46**, 173–200.
2. Steitz, J. A. (1977) in *Biological Regulation and Development*, ed. Goldberger, R. (Plenum, New York), in press.
3. Crick, F. H. C. (1966) *J. Mol. Biol.* **19**, 548–555.
4. Erdmann, V. A. (1976) *Prog. Nucleic Acid Res. Mol. Biol.* **18**, 45–90.
5. Lund, E. & Dahlberg, J. E. (1977) *Cell* **11**, 247–262.
6. Rich, A. & RajBhandary, U. L. (1976) *Annu. Rev. Biochem.* **45**, 805–860.
7. Jack, A., Ladner, J. E. & Klug, A. (1976) *J. Mol. Biol.* **108**, 619–649.
8. Peacock, A. C. & Dingman, C. W. (1967) *Biochemistry* **6**, 1818–1827.
9. Ikemura, T. & Dahlberg, J. E. (1973) *J. Biol. Chem.* **248**, 5024–5032.
10. Sanger, F., Brownlee, G. G. & Barrell, B. G. (1965) *J. Mol. Biol.* **13**, 373–389.
11. Barrell, B. G. (1972) in *Procedures in Nucleic Acids Research*, eds. Cantoni, G. L. & Davies, D. R. (Harper & Row, New York), Vol. 2, pp. 751–795.
12. Nishimura, S. (1972) *Prog. Nucleic Acid Res. Mol. Biol.* **12**, 49–85.
13. Dube, S. K., Marcker, K. A., Clark, B. F. C. & Cory, S. (1969) *Eur. J. Biochem.* **8**, 244–255.
14. Dube, S. K. & Marcker, K. A. (1969) *Eur. J. Biochem.* **8**, 256–262.
15. Herr, W. & Noller, H. F. (1975) *FEBS Lett.* **53**, 248–252.
16. Dahlberg, A. E., Dingman, C. W. & Peacock, A. C. (1969) *J. Mol. Biol.* **41**, 139–147.
17. Branlant, C., Sri Widada, J., Krol, A. & Ebel, J. P. (1977) *Nucleic Acids Res.*, **4**, 4323–4345.
18. Nomura, M., Lowry, C. V. & Guthrie, C. (1967) *Proc. Natl. Acad. Sci. USA* **58**, 1487–1493.
19. Crothers, D. M., Cole, P. E., Hilbers, C. W. & Shulman, R. G. (1974) *J. Mol. Biol.* **87**, 63–88.
20. Dube, S. K. (1973) *FEBS Lett.* **36**, 39–42.
21. Herr, W. & Noller, H. F. (1978) *Biochemistry*, in press.